

Experiment and Dynamic Simulations of Radiation Damping of Laser-Polarized Liquid ^{129}Xe at Low Magnetic Field in a Flow System

X. Zhou, J. Luo, X. Sun, X. Zeng, M. Zhan, S. Ding, and M. Liu

State Key Laboratory of Magnetic Resonance and Atomic and Molecular Physics,
Wuhan Institute of Physics and Mathematics, Chinese Academy of Sciences,
Wuhan, China

Received October 26, 2003

Abstract. Radiation damping is generally observed when a sample with high spin concentration and high gyromagnetic ratio is placed in a high magnetic field. However, we firstly observed liquid-state ^{129}Xe radiation damping with laser-enhanced nuclear polarization at low magnetic field in a flow system in which the polarization enhancement factor for the liquid-state ^{129}Xe was estimated to be 5000, and, furthermore, theoretically simulated the envelopes of the ^{129}Xe free induction decay and spectral lineshape in the presence of both relaxation and radiation damping with different pulse flip angles and ratios of T_2/T_{rd} . The radiation damping time constant T_{rd} of 5 ms was derived on the basis of the simulations. The reasons of depolarization and the further possible improvements were also discussed.

1 Introduction

Laser-polarized ^{129}Xe and ^3He gases [1] have found wide applications in polarized targets [2], magnetic resonance imaging (MRI) [3, 4], neutron polarization [5], fundamental symmetry studies [6], high-resolution nuclear magnetic resonance (NMR) spectroscopy [7], surface science [8], precision measurements [9], biological-system probe [10], quantum computer [11] and cross polarization to other nuclei [12, 13]. The enhanced NMR signals of laser-polarized ^{129}Xe , which are about 10^5 times larger than those from thermally polarized ^{129}Xe [1, 14], have opened the possibility to explore the radiation-damping effect [15] of laser-polarized ^{129}Xe .

Since Bloembergen and Pound [15] analyzed the physical process of radiation damping in 1954, radiation damping was noticed and studied for several years [16–19]. Although the research of radiation damping in NMR had almost halted from 1960 to 1988, it has once again evoked the interest of researchers in recent years because of the applications of high-field magnets and highly sensitive probes. Since then, a large number of research articles and reviews have been published [20–29].

Radiation damping is a nonlinear effect. The current induced by the transverse magnetization in the receiver radio-frequency (rf) coil interacts with the magnetization vector itself, tending to bring it back to the $+z$ -axis (the direction of the static magnetic field). Radiation damping is usually observed at high fields where liquid-phase magnetization M , the static magnetic field homogeneity, and the quality factor Q of the probe are sufficiently high [15, 16, 20]. The magnetization is $M = \gamma \hbar C P$ with respect to the Currie law, with γ being the gyromagnetic ratio, P the polarization, and C the spin concentration. In aqueous solutions the water proton concentration is usually 110 mol/l ($C \approx 110$ M), which is high enough to produce the radiation-damping effect. Radiation damping can also be observed for other solvents and concentrated samples [30]. According to the thermal polarization $P_0(B_0, T) \approx \gamma \hbar B_0 / (4\pi kT)$, either decreasing the temperature or increasing the magnetic field can enhance the polarization and make the radiation-damping effect stronger, but it can provide only limited relief. It is very natural to employ optical pumping and spin exchange [1] to improve the polarization.

Although radiation damping of laser-polarized gaseous xenon was obtained at 14 T on a Bruker DRX 600 spectrometer [31], the proper inversion of the magnetization could not be entirely interpreted with the dipolar field theory [32]. The dipolar field effects [33], on the other hand, could explain NMR instabilities and spectral clustering in laser-polarized liquid xenon [34]. In medical MRI, the existence of radiation damping both in the phantom experiments and in vivo affects the quality of imaging [35], and one can foresee that the same problem will emerge in the application of the lung MRI with hyperpolarized ^3He and ^{129}Xe [3]. Therefore until now, the microcosmic mechanism of radiation damping has still not been fully understood, and the corresponding dynamics problems need to be resolved.

Two recent articles [36, 37] have reported radiation damping of laser-polarized ^3He , which is easier to be observed than that of ^{129}Xe because the gyromagnetic ratio γ and optical pumping efficiency of ^3He are larger than those of ^{129}Xe . Here we report the first observation of radiation damping in laser-polarized liquid ^{129}Xe at the low magnetic field in a flow system, and the typical radiation-damped free induction decay (FID) envelopes and spectra at different pulse flip angles are presented and compared with theoretical ones. The characterization of such a system is important for hyperpolarized MRI at low magnetic fields [38]. Our experiment could provide another liquid-phase example to analyze the radiation-damping effect. In addition, laser-polarized liquid xenon and its radiation damping also have a number of potential applications, such as the construction of liquid xenon masers [39], the rapid and precise measurement of liquid xenon polarization [40], etc.

2 Experiment

The diagram of our experimental apparatus is shown in Fig. 1. The pump cell containing a few drops of metal Cs was maintained at approximately 333 ± 1 K by the resistance heater during optical pumping. The inner surfaces of the cylindrical

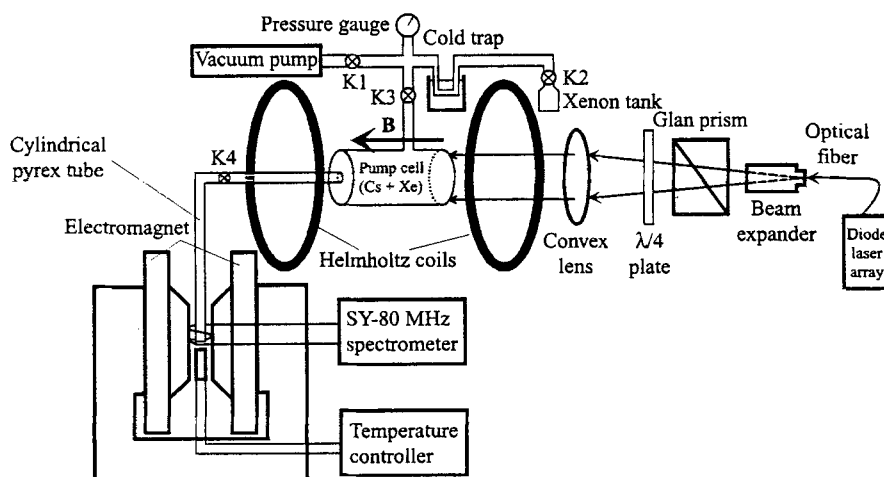


Fig. 1. Diagram of our experimental apparatus.

pyrex tube and the pump cell were coated with silane in order to slow down the relaxation of the ^{129}Xe upon collision with the tube wall. The cell was placed in a 25 G magnetic field generated by Helmholtz coils. The whole system was evacuated with the K2 valve closed and K1, K3 and K4 valves open. When the vacuum reached $1.5 \cdot 10^{-5}$ torr (100 torr = 13.3322 kPa), the valves K1, K4 were closed and K2, K3 were opened. The cell was filled with natural xenon gas (26% enriched ^{129}Xe gas) at 740 torr. After all the valves were closed, laser light from a 15 W laser array (Opto Power Co. Model OPC-D015-850-FCPS) at 852.1 nm was introduced to the system. The laser light resonates with the Cs D_2 transition line and induces an electron spin polarization in the Cs vapor via a standard optical pumping process [41]. The hyperpolarized ^{129}Xe gas was produced by spin-exchange collision at the same time. The polarization process took about 25 min. The K4 valve was then opened to allow the ^{129}Xe to be transmitted into the probe, precooled to 172 ± 1 K, of a Bruker SY-80M NMR spectrometer. The temperature of the probe was subsequently reduced to 160 ± 1 K to freeze the xenon into a condensed state. But the actual temperature, which was somewhat different from that of the monitor, was improved from the NMR observation that the solid-phase xenon and liquid-phase xenon coexist in the probe because the temperature range between the melting point and the boiling point of xenon was small ($4.6 \pm 3^\circ\text{C}$). To study radiation damping of the liquid ^{129}Xe , the sample was cooled down to 142 ± 1 K to completely freeze the xenon and then gradually warmed up and maintained at 166 ± 1 K.

3 Results and Discussion

Figure 2 shows the ^{129}Xe NMR time-domain signal and the corresponding spectrum at 160 ± 1 K when the 160° pulse was applied. The peak with a larger line

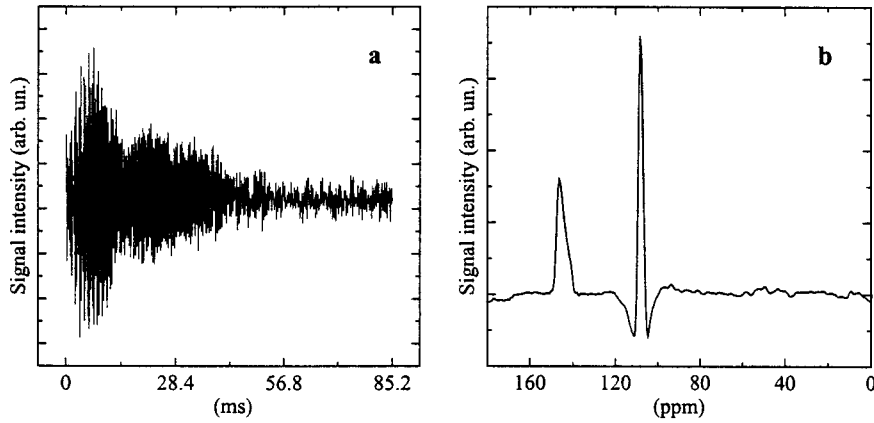


Fig. 2. Experimental ^{129}Xe FID signals of the liquid phase and the solid phase with radiation damping when the 160° pulse was applied (a) and the corresponding frequency spectrum (b).

width at high frequency ($\delta 147$) is assigned to solid ^{129}Xe and the sharp peak with phase distortion ($\delta 108$) is from liquid ^{129}Xe (Fig. 2b). Such phase distortion is the typical result of the radiation damping.

It should be noted that at 166 ± 1 K, only the liquid-state ^{129}Xe NMR signal at $\delta 108$ is observable. Figure 3 shows the ^{129}Xe FID signals and the corresponding frequency spectra excited by 60° , 90° , 120° , and 150° pulses. Compared with the theoretical FID envelope and spectrum for water in Fig. 4 [17, 23], these signals obviously indicated that the laser-polarized liquid ^{129}Xe has radiation-damping effects. Unlike the profile of the conventional FID (Fig. 3a1, a2), that of the typical radiation-damped FID excited by a pulse flip angle greater than 90° will increase initially and start to decay after reaching a maximum, and the position of the maximum is flip-angle-dependent (Fig. 3a3, a4). As it is expected, the amplitude of symmetrical phase-twisting of the corresponding spectra is enhanced when the flip angle is increased (Fig. 3b3, b4) [24, 25].

The strength of the radiation damping is characterized by the radiation damping time constant T_{rd} [16]. The longitudinal relaxation time T_1 of ^{129}Xe in the liquid phase is about 30 min [42, 43]. The transverse relaxation time T_2^* of ^{129}Xe in the NMR machine (Bruker SY-80M) due to the poor inhomogeneity is estimated to be 30 ms. Radiation damping can occur only when T_{rd} is shorter than T_2^* [24]. Compared with T_2^* and T_{rd} , the T_1 effect is negligible. The T_{rd} value can be estimated from the line width of the spectrum obtained by using very small pulse flip angle, since in this case the line shape will be reduced to a Lorentzian [25],

$$\Delta\nu_{1/2} = q/\pi T_2^* = \pi^{-1}(1/T_2^* + 1/T_{\text{rd}}).$$

Considering the error of $\Delta\nu_{1/2}$ and T_2^* , the T_{rd} values were in the range of 6 ± 2 ms. Then, according to the analytical results of the Bloch equations including only T_{rd} and T_2^* , which have been presented in ref. 25,

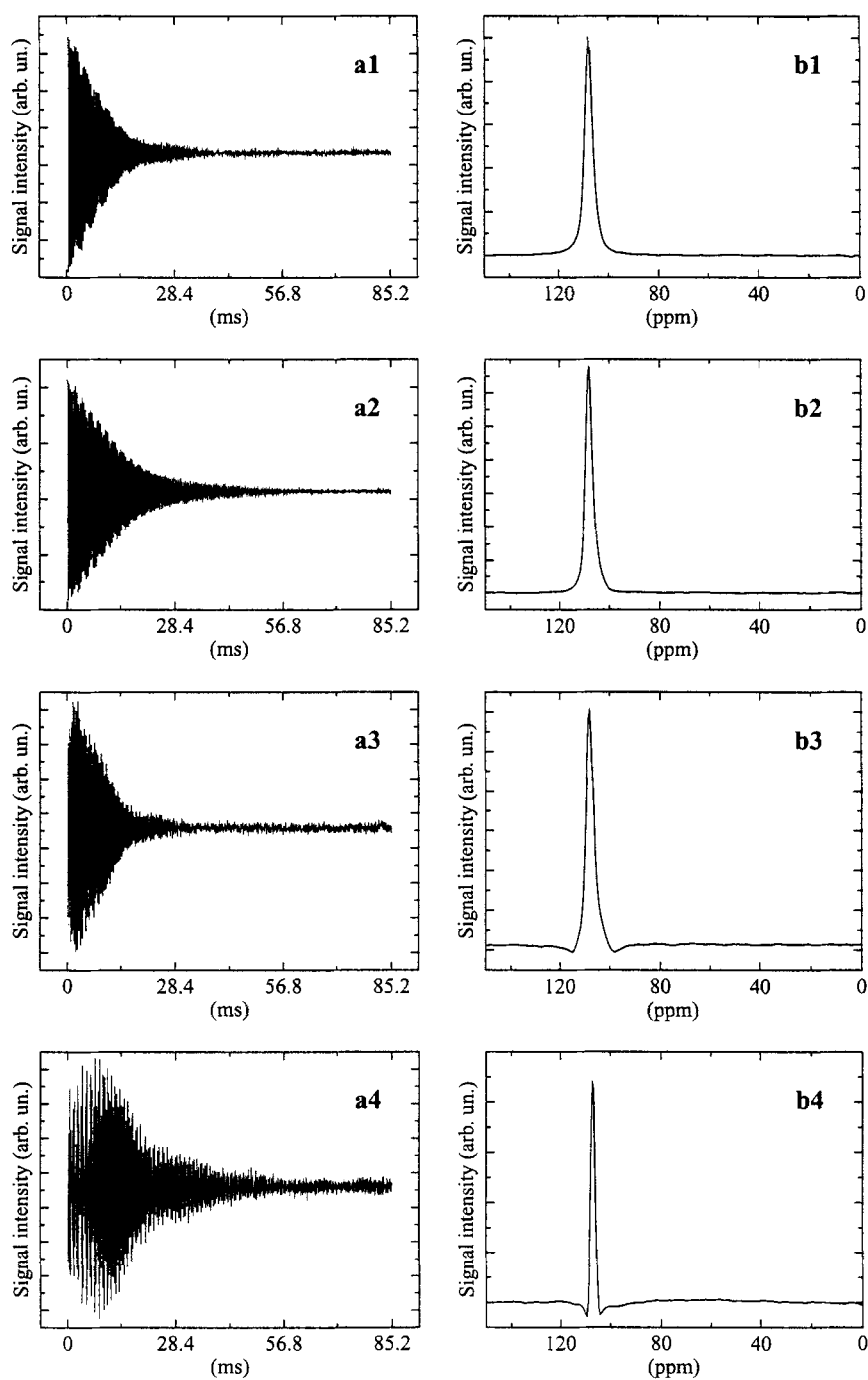


Fig. 3. Experimental liquid-phase ^{129}Xe FID signals when 60° (a1), 90° (a2), 120° (a3) and 150° (a4) pulses were applied and the corresponding frequency spectra (b1, b2, b3, b4).

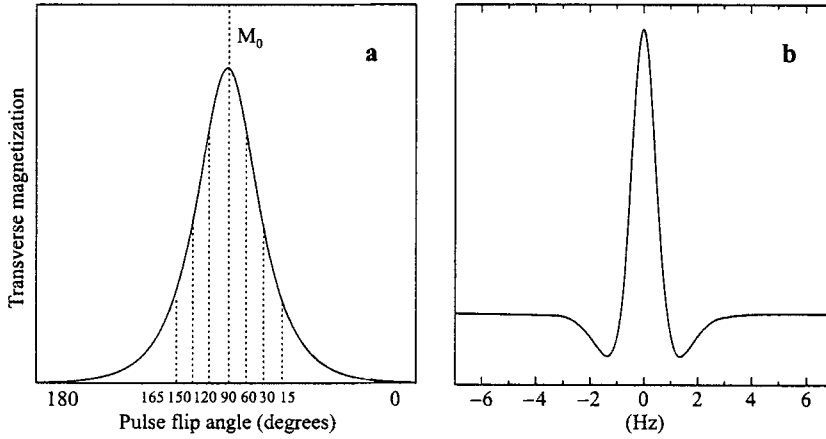


Fig. 4. **a** Envelope of FID with different flip angles under strong radiation damping. **b** The theoretical lineshape of water with strong radiation damping with a 150° flip pulse excitation, in which the T_{rd} of water proton was assumed to be 12 ms.

$$S(\omega) = 2M_0T_{rd} \frac{q}{T_2^*} \sum (-1)^n \frac{(2n+1)q/T_2^*}{((2n+1)q/T_2^*)^2 + \omega^2} \tan^{2n+1}(\eta/2), \quad 0 < \eta \leq \pi/2,$$

$$2M_0T_{rd} \frac{q}{T_2^*} \sum (-1)^n \frac{(2n+1)q/T_2^*}{((2n+1)q/T_2^*)^2 + \omega^2} (2\cos(\omega t_0) - \cot^{2n+1}(\eta/2)), \quad \pi/2 < \eta \leq \pi$$

with

$$q = (1 + (T_2^*/T_{rd})^2 + 2(T_2^*/T_{rd})\cos\theta_0)^{1/2},$$

$$t_0 = -(T_2^*/q)\tanh^{-1}(((T_2^*/T_{rd})\cos\theta_0 + 1)/q),$$

$$\cos\eta = ((T_2^*/T_{rd})\cos\theta_0 + 1)/q,$$

we simulated the spectra with different T_{rd} values and pulse flip angles in order to get the accurate T_{rd} value. The same simulation of the FID was performed with the formula [25]

$$M_y = (M_0T_{rd}/T_2^*)q\operatorname{sech}((q/T_2^*)(t - t_0)).$$

The T_2^* value of liquid-state ^{129}Xe was assumed to be 30 ms in all simulations unless otherwise indicated, which was the same as the experimental one. As a result, we found that the precise T_{rd} value of laser-polarized liquid ^{129}Xe was about 5 ms in our experiment. The simulated ^{129}Xe FID and the corresponding frequency spectrum, for a 150° pulse and $T_{rd} = 5$ ms, are shown in Fig. 5 and are in good agreement with our experimental results (Fig. 3a4, b4).

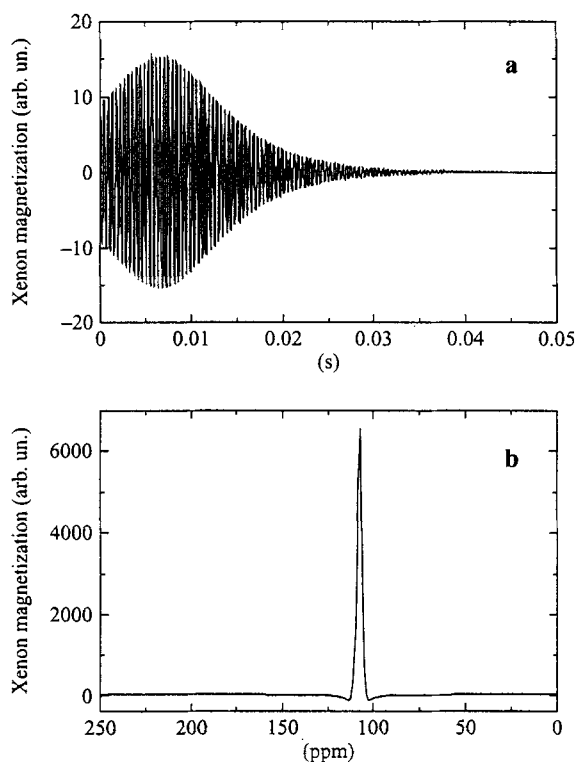


Fig. 5. Theoretically simulated ^{129}Xe FID (a) and corresponding frequency spectrum (b) when the 150° pulse was applied with $T_2^* = 30$ ms, and $T_{rd} = 5$ ms.

Figure 6 shows the simulated envelopes of the ^{129}Xe FID in the presence of relaxation and radiation damping with different flip angle pulses and T_{rd} values. From the spectra, we can learn that the envelope of the FID is associated with the ratio of T_2^*/T_{rd} and the flip angle θ_0 . If $T_2^*/T_{rd} \leq 1$, the bigger the ratio is, the faster the FID decays when $\theta_0 \leq 90^\circ$, contrary to the cases of $\theta_0 > 90^\circ$, and the radiation damping is impossible to occur and the maximum amplitude point is located at $t = 0$ whatever the flip angle θ_0 is. If $T_2^*/T_{rd} > 1$, the same situation occurs that the bigger the ratio is, the faster the FID decays, but when $\theta_0 > 90^\circ$ the FID rises at first and then declines after reaching the maximum amplitude point, which is higher when the ratio is bigger. The spectra also indicate that the FID decays monotonically when $\theta_0 \leq 90^\circ$, no matter what the ratio is. The radiation damping can be observed only when $T_2^*/T_{rd} > 1$ and when the pulse flip angle is greater than 90° . The bigger T_2^*/T_{rd} is, the stronger the radiation damping will be. The radiation damping will also occur even when $T_2^*/T_{rd} = 2$. So our observation of the liquid ^{129}Xe radiation damping under the conditions of the large ^{129}Xe magnetization and the ratio of $T_2^*(30 \text{ ms})/T_{rd}(5 \text{ ms}) = 6$ is reasonable.

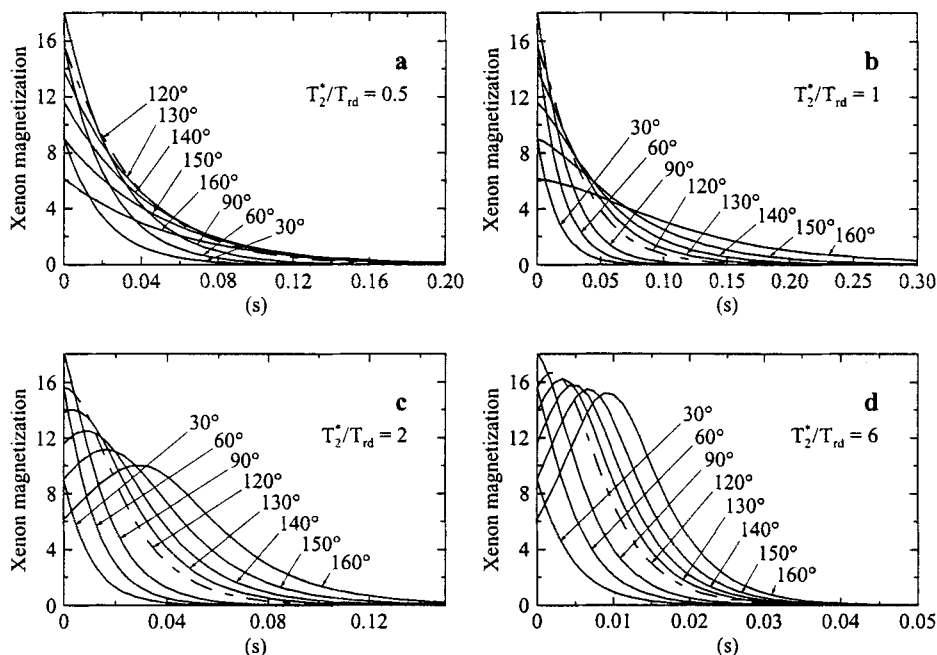


Fig. 6. Theoretical envelopes of the ^{129}Xe FID in the presence of relaxation ($T_2^* = 30$ ms) and radiation damping while the different pulse flip angles and T_{rd} were assumed: $T_{rd} = 60$ ms (a), $T_{rd} = 30$ ms (b), $T_{rd} = 15$ ms (c), and $T_{rd} = 5$ ms (d).

On the basis of the relation of the magnetization versus the nuclear spin polarization given by Abragam [19], and by comparison of the nuclear spin polarization P_L of ^{129}Xe produced by laser optical pumping with the Boltzmann polarization P_B of ^{129}Xe at the thermal equilibrium, the enhancement factor of the ^{129}Xe nuclear spin polarization can be expressed as

$$f = \frac{P_L}{P_B} = \frac{I_L}{I_B},$$

where I_L and I_B are the integral intensities of the measured NMR signals of the liquid ^{129}Xe under the conditions of the laser optical pumping and the thermal equilibrium, respectively. Therefore, the enhancement factor of the liquid ^{129}Xe was about 5000 on the basis of our measurement [44]. The Boltzmann polarization P_B of the ^{129}Xe at 166 K in the Bruker SY-80M (1.879 T) spectrometer is about $2.9 \cdot 10^{-6}$, hence the liquid-state ^{129}Xe nuclear spin polarization P_L is 1.45%, which was produced by spin exchange with laser-polarized Cs atoms at the low magnetic field of 25 G in a flow system.

Qualitatively, radiation damping emerges when the transverse relaxation time T_2^* is longer than the characteristic time of radiation damping

$$T_{\text{rd}} = \frac{1}{2\pi\eta Q M_{\gamma}}$$

[15, 16, 20], although the quality factors Q of our Bruker SY-80M NMR spectrometer is rather poor and the filling factor η is rather small, and the radiation damping effect is about four times more efficient in the case of protons than for ^{129}Xe nuclei at the same magnetization level because of the dependence of T_{rd} on the gyromagnetic ratio. But when the ^{129}Xe nuclear polarization is enhanced, the signal intensity of liquid ^{129}Xe is larger than that of water protons in a high magnetic field by comparing water protons signals at 11.7 T and room temperature ($C = 110 \text{ M}$, $P = 4.2 \cdot 10^{-5}$, $M = 7.83 \cdot 10^{-5} \text{ G/cm}^3$) with laser-polarized liquid ^{129}Xe signals ($C = 5.46 \text{ M}$, $P = 1.45 \cdot 10^{-2}$, $M = 3.69 \cdot 10^{-4} \text{ G/cm}^3$). The T_2^* value will be shortened dramatically due to the magnetic field inhomogeneity, so radiation damping of water protons could not be observed on the same SY-80M spectrometer, but with the enhancement of polarization, we have observed the liquid-phase radiation damping for our laser-polarized sample. The phenomenon that the radiation damping occurs for liquid ^{129}Xe but not for solid ^{129}Xe under the same polarization condition, also demonstrates that the radiation damping depends primarily on both the intensity of the magnetization and the characteristic time of radiation damping T_{rd} .

The polarization in a flow system is not so high as that in the close pump cell or that produced by the narrow-bandwidth Ti:sapphire laser [31]. The main causes are the following. (i) The loss of polarization is due to the magnetic field inhomogeneity during the transfer of laser-polarized ^{129}Xe gases. (ii) Since the bandwidth of our diode laser array is 3 nm but the absorbed bandwidth of Cs atom in the natural xenon at 740 torr is only 30 GHz, the efficient pump power is only about 0.125 W. (iii) The phase transition of laser-polarized ^{129}Xe can also bring about the depolarization. (iv) The relaxation of ^{129}Xe atoms at the walls still decreases the polarization, even though they were coated.

Thus we can see the further possible improvements in our experiment by adopting the following techniques: (i) creating the homogeneous magnetic field by two-layer solenoid with end correction coils, and keeping the transmission of laser-polarized xenon paralleling the static magnetic field; (ii) increasing the gas pressure of the pump cell in order to enhance the optically pumped absorbed power; (iii) decreasing the time of the phase transition of laser-polarized ^{129}Xe .

4 Conclusions

Usually, radiation damping was observed only when the sample has a high spin concentration, such as water protons, in the high magnetic field on a high-resolution spectrometer. However, our experiment indicated that under the condition of laser-enhanced nuclear polarization, which enhanced the liquid ^{129}Xe polarization to 5000 compared with that without optical pumping under the same conditions, the liquid ^{129}Xe radiation damping can also be observed even at low

magnetic field in a flow system. The liquid ^{129}Xe T_{rd} of our experiment was estimated with the help of the radiation damping line shape theory to be as short as 5 ms, and we theoretically simulated the FID and spectrum of ^{129}Xe in the presence of radiation damping and the transverse relaxation in order to compare them with the experimental ones. We also discussed whether the radiation damping would occur with different ratios of T_2^*/T_{rd} , and the theoretically simulated envelopes of the ^{129}Xe FID in the presence of both relaxation and radiation damping with different pulse flip angles and T_{rd} values were presented. The reasons of depolarization and the further possible improvements were also discussed. Furthermore, our experiment of laser-polarized liquid ^{129}Xe NMR may be a particularly good test bed for studying micromechanism of radiation damping.

Acknowledgements

This work was supported by the National Natural Science Foundation of China under Grant nr. 10234070, National Science Fund for Distinguished Young Scholars under Grant nr. 29915515 and National Fundamental Research Program under Grant nr. 2001CB309306. X.Z. is grateful to Xi-an Mao for helpful discussions and suggestions.

References

1. Walker T.G., Happer W.: *Phys. Rev. Lett.* **69**, 629–642 (1997)
2. Xu W., Dutta D., Xiong F., Anderson B., Auberbach L., Averett T., Bertozzi W., Black T., Calarco J., Cardman L., Cates G.D., Chai Z.W., Chen J.P., Choi S., Chudakov E., Churchwell S., Corrado G.S., Crawford C., Dale D., Deur A., Djawotho P., Filippone B.W., Finn J.M., Gao H., Gilman R., Glamazdin A.V., Glashauser C., Glöckle W., Golak J., Gomez J., Gorbenko V.G., Hansen J.-O., Hersman F.W., Higinbotham D.W., Holmes R., Howell C.R., Hughes E., Humensky B., Incerti S., Jager C.W., Jensen J.S., Jiang X., Jones C.E., Jones M., Kahl R., Kamada H., Kievsky A., Kominis I., Korsch W., Kramer K., Kumbartzki G., Kuss M., Lakuriqi E., Liang M., Liyanage N., LeRose J., Malov S., Margaziotis D.J., Martin J.W., McCormick K., McKeown R.D., McIlhany K., Meziani Z.-E., Michaels R., Miller G.W., Pace E., Pavlin T., Petratos G.G., Pomatsalyuk R.I., Pripstein D., Prout D., Ransome R.D., Roblin Y., Rvachev M., Saha A., Salmè G., Schnee M., Shin T., Slifer K., Souder P.A., Strauch S., Suleiman R., Sutter M., Tipton B., Todor L., Viviani M., Vlahovic B., Watson J., Williamson C.F., Witala H., Wojtsekhowski B., Yeh J., Zolnierczuk P.: *Phys. Rev. Lett.* **85**, 2900–2904 (2000)
3. Albert M.S., Cates G.D., Driehuys B., Happer W., Saam B., Springer C.S. Jr, Wishnia A.: *Nature* **370**, 199–201 (1994)
4. Eberle B., Weiler N., Markstaller K., Kauczor H.-U., Deninger A., Ebert M., Grossmann T., Heil W., Lauer L.O., Roberts T.P.L., Schreiber W.G., Surkau R., Dick W.F., Otten E.W., Thelen M.: *J. Appl. Physiol.* **87**, 2043–2052 (1999)
5. Jones G.L., Gentile T.R., Thompson A.K., Chowdhuri Z., Dewey M.S., Snow W.M., Wietfeldt F.E.: *Nucl. Instrum. Methods Phys. Res. Sect. A* **440**, 772–776 (2000)
6. Rosenberry M.A., Chupp T.E.: *Phys. Rev. Lett.* **86**, 22–25 (2000)
7. Raftery D., Long H., Meersmann T., Grandinetti P.J., Reven L., Pines A.: *Phys. Rev. Lett.* **66**, 584–587 (1991)
8. Pietrass T., Bifone A., Pines A.: *Surf. Sci.* **334**, L730–L734 (1995)
9. Bear D., Stoner R.E., Walsworth R.L., Kostelecký V.A., Lane C.D.: *Phys. Rev. Lett.* **85**, 5038–5041 (2000); Bear D., Stoner R.E., Walsworth R.L., Kostelecký V.A., Lane C.D.: *Phys. Rev. Lett.* **89**, 209902-1 (2002)

10. Rubin S.M., Spence M.M., Pines A., Wemmer D.E.: *J. Magn. Reson.* **152**, 79–86 (2001)
11. Verhulst A.S., Liivak O., Sherwood M.H., Vieth H.M., Chuang I.L.: *Appl. Phys. Lett.* **79**, 2480–2482 (2001)
12. Driehuys B., Cates G.D., Happer W., Mabuchi H., Saam B., Albert M.S., Wishnia A.: *Phys. Lett. A* **184**, 88–92 (1993)
13. Long H.W., Gaede H.C., Shore J., Reven L., Bowers C.R., Kritzenberger J., Pietrass T., Pines A., Tang P., Reimer J.A.: *J. Am. Chem. Soc.* **115**, 8491–8492 (1993)
14. Sun X., Hu H., Zeng X.: *Appl. Magn. Reson.* **16**, 363–372 (1999)
15. Bloembergen N., Pound R.V.: *Phys. Rev.* **95**, 8–12 (1954)
16. Bloom S.: *J. Appl. Phys.* **28**, 800–805 (1957)
17. Szoeké A., Meiboom S.: *Phys. Rev.* **113**, 585–586 (1959)
18. Bruce C.R., Norberg R.E., Pake G.E.: *Phys. Rev.* **104**, 419–420 (1956)
19. Abragam A.: *The Principles of Nuclear Magnetism*, p. 264. Oxford: Clarendon 1961.
20. Warren W.S., Hames S.L., Bates J.L.: *J. Chem. Phys.* **91**, 5895–5904 (1989)
21. Jeener J., Vlassenbroek A., Broekaert P.: *J. Chem. Phys.* **103**, 1309–1332 (1995)
22. Vlassenbroek A., Jeener J., Broekaert P.: *J. Chem. Phys.* **103**, 5886–5897 (1995)
23. Mao X.A., Wu D., Ye C.H.: *Chem. Phys. Lett.* **204**, 123–127 (1993)
24. Mao X.A., Ye C.H.: *J. Chem. Phys.* **99**, 7455–7462 (1993)
25. Mao X.A., Guo J.X., Ye C.H.: *Phys. Rev. B* **49**, 15702–15711 (1994)
26. Guo J.X., Mao X.A.: *J. Phys. II France* **6**, 1183–1193 (1996)
27. Chen J.H., Mao X.A., Ye C.H.: *J. Magn. Reson. A* **123**, 126–130 (1996)
28. Chen J.H., Mao X.A., Ye C.H.: *J. Magn. Reson.* **124**, 490–494 (1997)
29. Chen J.H., Mao X.A.: *Chem. Phys. Lett.* **274**, 549–553 (1997)
30. Mao X.A., Guo J.X., Ye C.H.: *Chem. Phys. Lett.* **222**, 417–421 (1994)
31. Berthault P., Desvaux H., Go G.L., Pétero M.: *Chem. Phys. Lett.* **314**, 52–56 (1999)
32. Warren W.S., Richter W., Andreotti A.H., Farmer B.T. II: *Science* **262**, 2005–2009 (1993)
33. Jeener J.: *Phys. Rev. Lett.* **82**, 1772–1775 (1999)
34. Sauer K.L., Marion F., Nacher P.J., Tastevin G.: *Phys. Rev. B* **63**, 184427–1–184427–4 (2001)
35. Zhou J., Susumui M., van Zijl P.C.M.: *Magn. Reson. Med.* **40**, 712–719 (1998)
36. Wong G.P., Tseng C.H., Pomeroy V.R., Mair R.W., Hinton D.P., Hoffmann D., Stoner R.E., Hersman F.W., Cory D.G., Walsworth R.L.: *J. Magn. Reson.* **141**, 217–227 (1999)
37. Gentile T.R., Rich D.R., Thompson A.K., Snow W.M., Jones G.L.: *J. Res. Natl. Inst. Stand. Technol.* **106**, 709–729 (2001)
38. Wong-Foy A., Saxena S., Moulé A.J., Bitter H.L., Seeley J.A., McDermott R., Clarke J., Pines A.: *J. Magn. Reson.* **157**, 235–241 (2002)
39. Rosenberry M.A., Chupp T.E.: *Phys. Rev. Lett.* **86**, 22–25 (2001)
40. Verhulst A.S., Liivak O., Sherwood M.H., Chung I.L.: *J. Magn. Reson.* **155**, 145–149 (2002)
41. Zeng X., Wu Z., Call T., Miron E., Schreiber D., Happer W.: *Phys. Rev. A* **31**, 260–278 (1985)
42. Moschos A., Reisse J.: *J. Magn. Reson.* **95**, 603–606 (1991)
43. Stith A., Hitchens T.K., Hinton D.P., Berr S.S., Driehuys B., Brookeman J.R., Bryant R.G.: *J. Magn. Reson.* **139**, 225–231 (1999)
44. Zhou X., Luo J., Sun X., Zeng X., Liu M., Liu W.: *Acta Phys. Sin.* **51**, 2221–2224 (2002) (in Chinese)

Authors' address: Xin Zhou, State Key Laboratory of Magnetic Resonance and Atomic and Molecular Physics, Wuhan Institute of Physics and Mathematics, Chinese Academy of Sciences, P. O. Box 71010, Wuhan 430071, People's Republic of China
E-mail: xinzhou@wipm.ac.cn